

A SPRING-MASS-DAMPER MODEL OF BIPEDAL WALKING TO SIMULATE GROUND REACTION FORCES PRODUCED BY HUMANS

Dianelys Vega

Carlos Magluta

Ney Roitman

dianelys@coc.ufrj.br

magluta@coc.ufrj.br.com

roitman@coc.ufrj.br

Laboratory of Structures (LabEst)–PEC/COPPE/UFRJ

Federal University of Rio de Janeiro, Technology Center, Block I-216, Ilha do Fundão, 21941-9726, Rio de Janeiro, Brazil

Abstract. The pedestrian-bridge dynamic interaction problem has been the focus of significant research worldwide due to the increase in vibration problems of footbridges caused by walking pedestrians. On this topic, several authors have proposed biomechanical models to represent the pedestrian. However, turning these models practical for use in engineering is still a challenge as numerous experimental results are needed to validate them and identify their parameters. In this research, a numerical model of bipedal walking with stiffness and damping was implemented in MATLAB. In parallel, experimental tests involving different volunteers were carried out at the Structures Laboratory of COPPE/UFRJ (LabEst). The volunteers were asked to walk at three different speeds on a test structure. The step forces were measured by instrumented force plates and the acceleration nearest to the pedestrian's center of mass by using an accelerometer placed on a belt attached at the waist of each subject. In order to validate this model, the simulated ground reaction forces (GRFs) were correlated with the experimental measurements obtained from force plates, and thus the model parameters were identified. A large number of Monte Carlo simulations were performed to find the best numerical-experimental correlation for each case. This work intends to provide a database of parameters for a bipedal walking model aiming the future use of this model in practice.

Keywords: bipedal walking models, human induced loads, vibrations

1 Introduction

The simulation of loads induced by walking pedestrians has been studied for many authors during the last decades due to the increasing evidence of the existence of interaction between pedestrians and structures. Numerous models have been proposed in literature in order to replicate human walking as close as possible. Since human body is extremely complex, different levels of simplification are introduced, resulting in models with different levels of complexity [1]-[2].

The most commonly used model in literature is the linear spring-mass-damper model (SMD), in which the human body is represented by one or more lumped masses, linearly connected by springs and dampers [3]. The biomechanical properties of the human body are difficult to obtain due to the complexity of mechanisms involved during walking and the inter and intra-subject variabilities. However, there already exists in literature some attempts to estimate them. Da Silva and Pimentel [3] identified the parameters of a one degree of freedom spring-mass-damper model through the correlation of GRF and center of mass acceleration amplitudes with experimental measures, and proposed empirical equations for mass, stiffness, and damping of the model. Other contributions can be found in the works conducted by Toso *et.al.* [4] and Shahabpoor *et.al.* [5].

Although the SMD model has shown a good correlation when compared to experimental measures, a disadvantage is the two phases of the gait cycle are not represented, that is, the load over time is always applied at a single point, not being possible the directly determining of GRFs. However, it opened up the path for describing the human body dynamics and brought important contributions to the development of more sophisticated models, such as the bipedal walking models.

Bipedal walking models were developed to represent the gait cycle in more detail. Although, they are based on some simplifications of walking, have shown great capacity to represent the patterns of human locomotion, and an important feature is GRFs can be directly obtained. The simplest bipedal model is the inverted pendulum-inspired model [6]. It consists of a point of mass on top, in which the total mass of the human body is lumped, and two massless straight lines, representing the legs. According to Dang and Živanović [7] it represents the kinematics of the center of mass better than the linear SMD model. More sophisticated models emerged as the result of adding springs and dampers to the inverted pendulum [8], [9]. There are only a few attempts of identifying parameters for bipedal models, among them can be found the works conducted by Dang [10] and Li *et.al.*[11], in which experimental data corresponding to 10 and 9 test subjects respectively was used to correlate with numerical simulations in order to identify range of values for parameters. Therefore, there is still a need for researches related to validation of bipedal walking models with experimental measures.

The present paper aims to validate a spring-mass-damper model of bipedal walking with stiffness and dampers [9] with a comprehensive data set of experimental tests performed for this purpose. The model parameters were identified through the correlation between the simulated GRFs and the experimental measurements. To this end, a great number of Monte Carlo simulations were realized.

2 Pedestrian model

The pedestrian is represented by a lumped mass at its center of mass and two massless and compliant legs with a stiffness, a time variant-damper and equal rest length L_0 [9], as shown in Fig.1.

A step cycle is defined between two successive heel impacts of the same foot, and is divided in a single support phase, when only one foot is in contact with the ground and a double support phase, when the two feet are in contact with the ground. The double support phase begins when the unsupported foot, from now on referred to as the trailing leg, touches down the floor and ends when the supported foot, from now on referred to as the leading leg, touches off. That means that the trailing leg is repositioned ahead of the body's center of mass and becomes the leading leg for the next step cycle. The single support phase ends when the trailing leg hits the ground. The angle with which the leg touches down at the initial moment of the double support phase is called as angle of attack θ_0 .

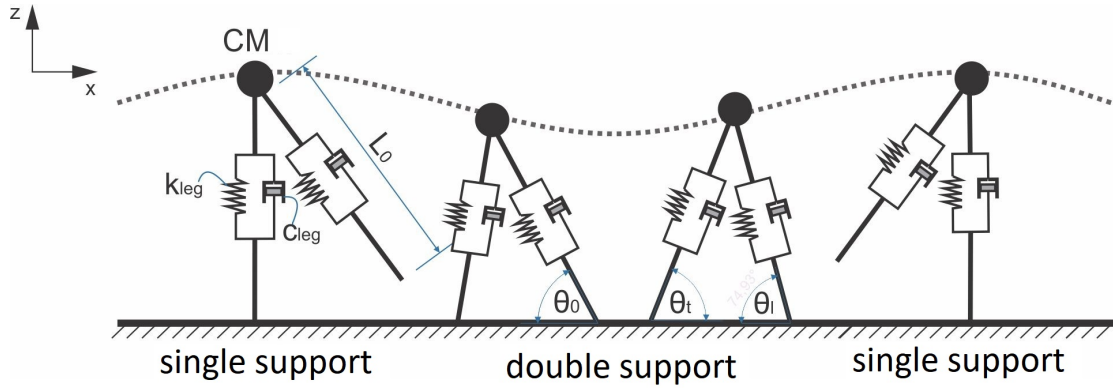


Figure 1. Schematic of the pedestrian biomechanical walking model

2.1 Equation of motion of the pedestrian body

The longitudinal and vertical displacements of the center of mass are expressed in Cartesian coordinates x, z . The walking speed is considered constant in order to simplify the mathematical model as this research is only focused on loads in vertical direction. Therefore, the pedestrian's motion can be described by a linear equation in the x -direction and by a non-linear equation in the z -direction. The equilibrium equation for the pedestrian body in z -direction is expressed by

$$m_h \ddot{z} + (F_{s,l} + F_{d,l}) \sin \theta_l - (F_{s,t} + F_{d,t}) \sin \theta_t + m_h g = 0 \quad (1)$$

where $F_{s,l}, F_{s,t}$ are the elastic forces, $F_{d,l}, F_{d,t}$ the damping forces, corresponding to leading and trailing legs respectively, $m_h \ddot{z}$ is the inertial force and $m_h g$ the gravitational force, corresponding to the center of mass.

The elastic forces are given by

$$\begin{aligned} F_{s,l} &= k_{leg} (L_l(t) - L_0) \\ F_{s,t} &= k_{leg} (L_t(t) - L_0) \end{aligned} \quad (2)$$

and the damping forces can be expressed as

$$\begin{aligned} F_{d,l} &= \alpha(t) c_{leg} v_l \\ F_{d,t} &= (1 - \alpha(t)) c_{leg} v_t \end{aligned} \quad (3)$$

where $L_l(t)$ and $L_t(t)$ are the lengths of the leading and trailing legs at a given time t , c_{leg} and k_{leg} are the leg damping and leg stiffness, and v_l and v_t are the axial spring velocities of the legs.

The leg lengths can be determined by

$$\begin{aligned} L_l(t) &= \sqrt{(n_s l_s - x)^2 + z^2} \\ L_t(t) &= \sqrt{(x - (n_s - 1) l_s)^2 + z^2} \end{aligned} \quad (4)$$

where l_s is the step length and n_s is the step number, $\alpha(t)$ is the damping coefficient and goes from zero at the beginning of the double support phase to one at the beginning of the single support phase.

During the double support phase $\alpha(t)$ can be calculated as:

$$\alpha(t) = \frac{L_t(t) - L_t(0)}{L_0 - L_t(0)} \quad (5)$$

The axial spring velocities can be obtained from the derivative of the equations of the leg lengths as

$$\begin{aligned} v_l &= \frac{d}{dt} L_l(t) = \frac{-(n_s l_s - x)\dot{x} + z\dot{z}}{\sqrt{(n_s l_s - x)^2 + z^2}} = -\dot{x} \cos \theta_l + \dot{z} \sin \theta_l \\ v_t &= \frac{d}{dt} L_t(t) = \frac{(x - (n_s - 1)l_s)\dot{x} + z\dot{z}}{\sqrt{(x - (n_s - 1)l_s)^2 + z^2}} = \dot{x} \cos \theta_t + \dot{z} \sin \theta_t \end{aligned} \quad (6)$$

By substituting Eq.4 in Eq.2 and Eq.6 in Eq.3:

$$\begin{aligned} F_{s,l} &= k_{leg} \left(\sqrt{(n_s l_s - x)^2 + z^2} - L_0 \right) \\ F_{s,t} &= k_{leg} \left(\sqrt{(x - (n_s - 1)l_s)^2 + z^2} - L_0 \right) \end{aligned} \quad (7)$$

$$\begin{aligned} F_{d,l} &= \alpha(t)c_{leg}(-\dot{x} \cos \theta_l + \dot{z} \sin \theta_l) \\ F_{d,t} &= (1 - \alpha(t))c_{leg}(-\dot{x} \cos \theta_t + \dot{z} \sin \theta_t) \end{aligned} \quad (8)$$

and substituting Eq.2 and Eq.8 in Eq.1 we obtain the equation of motion of the pedestrian in the z direction

2.2 Ground reaction force

The total elastic and damping forces acting on the direction of each leg are calculated by the equations 2 and 3 . Thus, the GRF corresponding to each leg in the z -direction is calculated by

$$\begin{aligned} GRF_l &= (F_{s,l} + F_{d,l}) \sin \theta_l \\ GRF_t &= (F_{s,t} + F_{d,t}) \sin \theta_t \end{aligned} \quad (9)$$

When in the single support phase $GRF_t = 0$.

2.3 Simulation of human walking

The pedestrian was considered walking in a straight line in a rigid surface. The equations given in section 2.1 were implemented in MATLAB, and the procedure to obtain the time response is described in the following steps:

- 1 The geometrical and physical pedestrian parameters, such as: weight of the human body, leg stiffness, damping leg, walking speed, step length, rest length of the leg are established.
- 3 The initial conditions of the center of mass of the pedestrian are set.
- 4 The overall mass, stiffness and damping matrices at time $t = 0$ are assembled.
- 5 The initial acceleration of the system is computed using the equilibrium force equation:
$$\ddot{z}_0 = m_h^{-1} (F_0 - c\dot{z}_0 - k_0)$$
- 6 For each time step the following time integration procedure is performed:
 - 6.1 The position of the two feet is determined by
$$x_l = n_s d_i, \quad x_t = (n_s - 1) d_i$$
where n_s is the step number and d_i the step length.
 - 6.2 The effective vertical stiffness and damping are then computed.
 - 6.3 The overall mass, damping, stiffness matrices and force vector are assembled.
 - 6.4 The displacement, velocity and acceleration at the end of the time increment are determined applying the 4th order Runge-Kutta method.
 - 6.5 The step cycle is checked by comparing the length of the trailing leg $L_t(t)$ with the rest length of the leg L_0 . If the length of the trailing leg is larger than the rest length of the leg the cycle is in the single support phase, otherwise in the double support phase.

- 6.6 If $L_t(t) > L_0$, the distance between the center of mass and the contact point for the next step cycle is computed. When the distance between the center of mass and the next contact point equals the rest length of the leg, the step number is set to $n_s = n_s + 1$.
- 6.7 The procedure described in steps 6.1 to 6.7 is repeated to obtain the dynamic response of the system for the next time step until the end of the time history.

3 Experimental tests

Experimental tests were carried out on a prototype footbridge at the Structures Laboratory (LabEst) of Federal University of Rio de Janeiro (COPPE-UFRJ). The structure consists of a reinforced concrete slab of 12,20 m x 2,20 m x 0,10 m dimensions over longitudinal and transverse steel beams. For this test campaign, it was placed directly over the floor in order to turn it into a rigid surface. More details of the test structure can be found in Faisca [12] and Vega [13].

The acquisition of experimental data was realized using an acquisition system with software that allows controlling test's parameters such as calibration constants, active channels, cutoff frequency, sampling frequency, etc. The instrumentation consisted of force plates with dimensions of 0,90 m x 0,90 m, placed directly over the structure and covering its entire surface area. Seven force plates were connected to the acquisition system to measure the step forces in the vertical direction. The acceleration close to the pedestrian's center of mass was measured by an accelerometer placed on a belt attached to the pedestrian's waist. After the acquisition, the experimental signals were processed and filtered with a Moving Average filter.

During the tests, volunteers were asked to walk on the structure at three different walking speeds: slow, normal and fast. The pedestrians' natural walking pace has been respected, i.e., no restrictions have been imposed to control their walking speed. Each volunteer made a round trip three times for each walking pace. In Fig. 2 is shown a typical pedestrian path during the tests. The physical parameters of each subject such as mass, height, leg length, the center of mass height and others were measured before conducting the tests and are shown in Table 1. In this paper is presented experimental data corresponding to 27 test subjects.

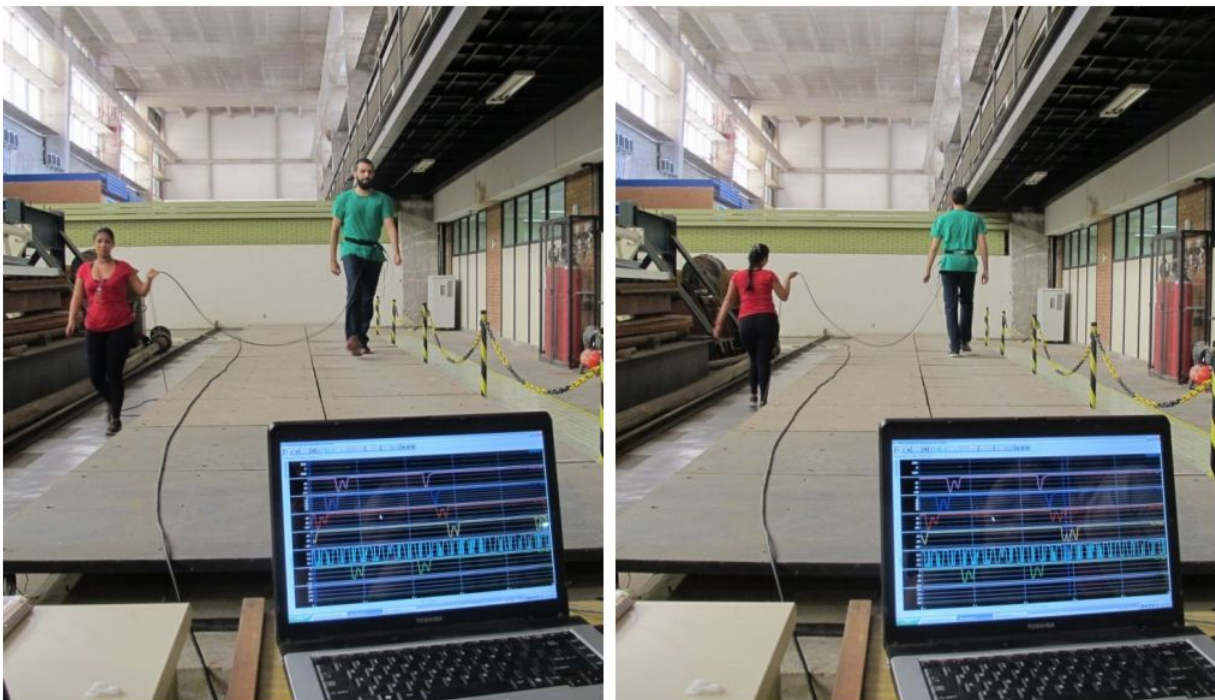


Figure 2. Typical pedestrian path during the tests

Table 1. Characteristics of pedestrians

Subject	Gender	Age	h (m)	h_{CM} (m)	L (m)	W (kg)	Shoes	Size shoes
1	F	31	1,60	0,97	0,87	65,6	tennis shoes	35
2	F	58	1,63	0,97	0,80	52,0	ballet flats	36
3	M	23	1,75	1,02	0,98	69,4	tennis shoes	38
4	M	22	1,75	1,03	0,98	63,7	tennis shoes	42
5	F	27	1,60	1,02	0,83	55,5	ballet flats	37
6	F	29	1,60	0,98	0,78	59,1	sandals	35
7	M	43	1,72	1,06	0,90	84,4	tennis shoes	42
8	M	28	1,72	0,99	0,90	102,6	tennis shoes	41
9	M	25	1,72	1,02	0,90	60,0	tennis shoes	40
10	M	26	1,70	1,04	0,89	65,2	tennis shoes	41
11	F	27	1,68	1,06	0,90	55,5	ballet flats	39
12	F	32	1,65	0,98	0,81	55,0	ballet flats	36
13	F	32	1,70	1,03	0,84	72,7	sandals	37
14	F	29	1,48	0,86	0,73	39,8	espadrilles	33
15	M	33	1,88	1,12	0,99	108,3	boots	44
16	M	31	1,79	1,10	0,97	75,3	sneakers	41
17	M	26	1,79	1,05	0,92	69,7	sneakers	42
18	M	33	1,74	1,08	0,92	68,5	tennis shoes	40
19	F	31	1,66	1,00	0,86	73,0	tennis shoes	37
20	M	33	1,74	1,05	0,92	80,8	tennis shoes	41
21	M	30	1,68	1,00	0,88	74,7	tennis shoes	41
22	M	31	1,72	1,06	0,90	82,3	sneakers	41
23	M	31	1,84	1,04	1,00	77,9	sneakers	41
24	M	22	1,74	1,08	0,98	66,9	boots	41
25	M	32	1,82	1,13	1,00	88,4	tennis shoes	42
26	M	29	1,80	1,11	0,92	73,4	tennis shoes	40
27	F	21	1,74	1,05	0,91	76,8	tennis shoes	38

The step frequency and average walking speed of each pedestrian at each walking speed were estimated from experimental tests. The step frequency was obtained through the frequency spectrum of CM's acceleration signal, using a program developed in LabEst (COPPE /UFRJ) in LabVIEW programming tool. The walking speed at each trial was calculated knowing the distance traveled by the pedestrian and initial and final instant times recorded by the first and the last force plates. For each pace was defined a speed value considered as the average walking speed of all trials performed at that pace. The mean

values and standard deviations of step frequency and walking speed found for slow, normal and fast walking pace are $1,60\text{Hz}\pm 0,17$, $1,83\text{Hz}\pm 0,12$, $2,14\text{Hz}\pm 0,13$ and $0,91\text{m/s}\pm 0,11$, $1,17\text{m/s}\pm 0,12$, $1,66\text{m/s}\pm 0,21$ respectively.

4 Monte Carlo Simulations

The input parameters of the model are the human body mass (m_h), the leg stiffness (k_{leg}), the leg damping, (ξ_{leg}), the step frequency (f_s), the walking speed (w_s), the rest length of the leg (L_0) and the attack angle (θ_0). Initial velocity in the vertical direction when considered close to zero does not generate instability during the time integration process. The values for input parameters are adopted as follows:

- m_h is fixed as the measured pedestrian mass in kg.
- L_0 is 20 % larger than actual leg length, based on data from literature ([10]).
- θ_0 is also adopted from values found in literature between $70 - 75^\circ$ ([10]), but it is adjusted through the integration process.
- f_s is the inverse of the period, which is estimated from experimental measurements of GRFs time history.
- w_s is established as the calculated experimental mean value from tests.
- k_{leg} and ξ_{leg} are assumed to be approximately 15-25kN/m and 5-8% respectively, from the biomechanical literature ([9], [10]).

In a first attempt, the model parameters were manually fitted through a trial and error process, but due to the variety of possible parameter combinations, Monte Carlo simulations were performed to find the best possible correlation between numerical and experimental GRFs. There were performed 5000 or 10000 simulations per case, depending on the walking speed. For faster walking speeds a greater number of simulations was needed to achieve good correlations. A strategy was established to find the best correlations as possible based on the smallest errors. Two types of error were considered, error in coordinates, ie the force value at each time instant, and the stance time, both calculated according to Eq.10. The total error is given by Eq.11.

$$E_i = \text{abs} \left(\frac{Exp - Num}{Exp} \right) \quad (10)$$

$$E_t = \sum_{i=1}^{ne} \left(\frac{E_i}{ne} \right) \quad (11)$$

After simulations, 20 parameter combinations corresponding to the smallest total and stance time errors simultaneously were chosen. The average values and standard deviations for this set of parameters were calculated and since there was little variation between them, they were assumed as the model parameters for the analyzed case.

5 Results and discussion

The procedure described in section 4 was used to estimate model parameters for all test subjects at each walking speed but it was not possible to find good correlations for all of them. Due to the fact that pedestrians were asked to walk in their natural way, in some attempts, it was not possible to obtain a complete step force signal. The tests with less than three adequate force signals were not considered. Also, in some cases, the force signals presented high levels of noise.

In addition, the numerical model was not efficient for speeds faster than 1,5m/s. Thus, only those attempts at lower speeds could be simulated. In total, were found good correlations at the three analyzed walking speeds for 16 pedestrians. In Table 2 are shown the model parameters found for subject 1 along

Table 2. Model parameters of subject 1

Walking pace	Tests		Model						
	w_s (m/s)	f_s (Hz)	L_0 (m)	m_h (kg)	w_s (m/s)	f_s (Hz)	k_{leg} (kN/m)	ξ_{leg} (%)	θ_0
slow	1,00	1,78	1,07	65,6	1,07	1,90	18,0	6,8	70,9 ⁰
normal	1,21	1,95	1,16	65,6	1,20	2,04	21,6	6,6	72,4 ⁰
fast	1,51	2,25	1,19	65,5	1,48	2,31	23,2	5,5	71,6 ⁰

Actual leg length and pedestrian mass are $L = 0,87\text{m}$ e $m_h = 65,6\text{kg}$ respectively.

with the corresponding experimentally measured parameters.

Figure 3 presents the correlation between step frequency and walking speed of the model and the ones experimentally estimated. Equations 12 and 13 express the linear regression equation for walking speed and step frequency with R^2 values of 0,92 and 0,93 respectively. The equations were found with 59 samples.

$$w_{s(mod)} = 0,7367w_{s(exp)} + 0,2908 \quad (12)$$

$$f_{s(mod)} = 1,1293f_{s(exp)} - 0,1472 \quad (13)$$

In Fig.4 is shown the numerical-experimental correlation of GRFs and CM's acceleration of subject 1 at the three walking speeds. As can be observed in the figure, the simulated GRF presented a very good correlation with the experimental measured, being better for slower walking speeds. This trend was also observed from the results obtained for other pedestrians. These findings are in agreement with Kim and Park [14].

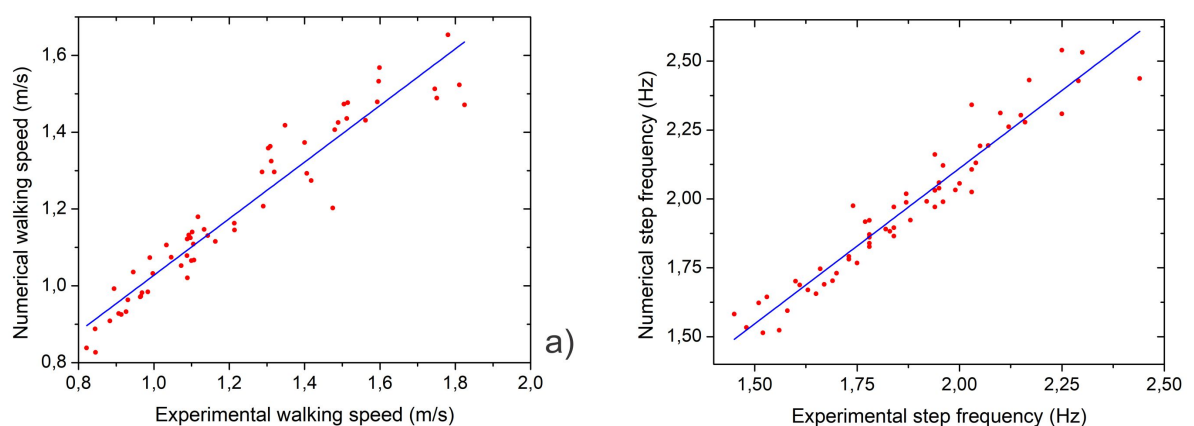


Figure 3. Experimental-numerical correlation of step frequency and walking speed

In Fig.5 is presented the variation of the rest length of the leg L_0 , the leg stiffness k_{leg} and the damping leg ξ_{leg} with walking speed. The results show that rest length and leg stiffness increase with increasing speed, however, the damping leg does not show a clear trend.

The rest length of the leg was for all cases longer than the actual leg length, increasing with speed, but in average 20-30% longer than the actual leg length, in agreement with findings of Dang [10]. The

range for the leg stiffness values of the entire population studied was between 12-33kN/m, but in most cases between 15-26kN/m, in agreement with the ranges proposed in the biomechanical literature. The values outside this range correspond to people with body mass lower or higher than the average. The leg damping values for the entire population remained between 5-13%, but in most cases between 6-10%, also agreeing with the range found in literature.

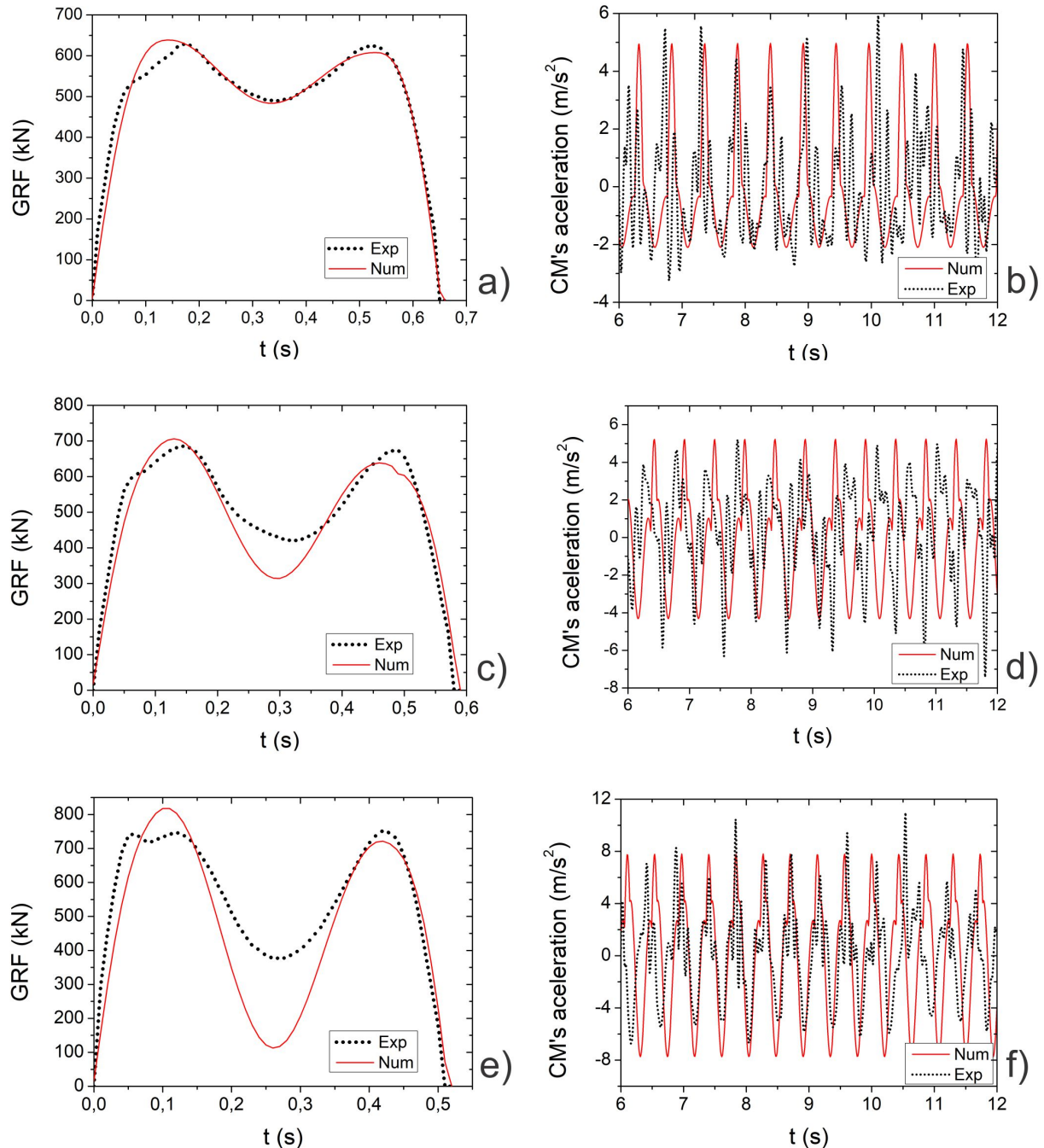


Figure 4. Best correlation of GRF and CM's acceleration of test subject 1 obtained from MC simulations, a)-b) slow, c)-d) normal and e)-f) fast walking.

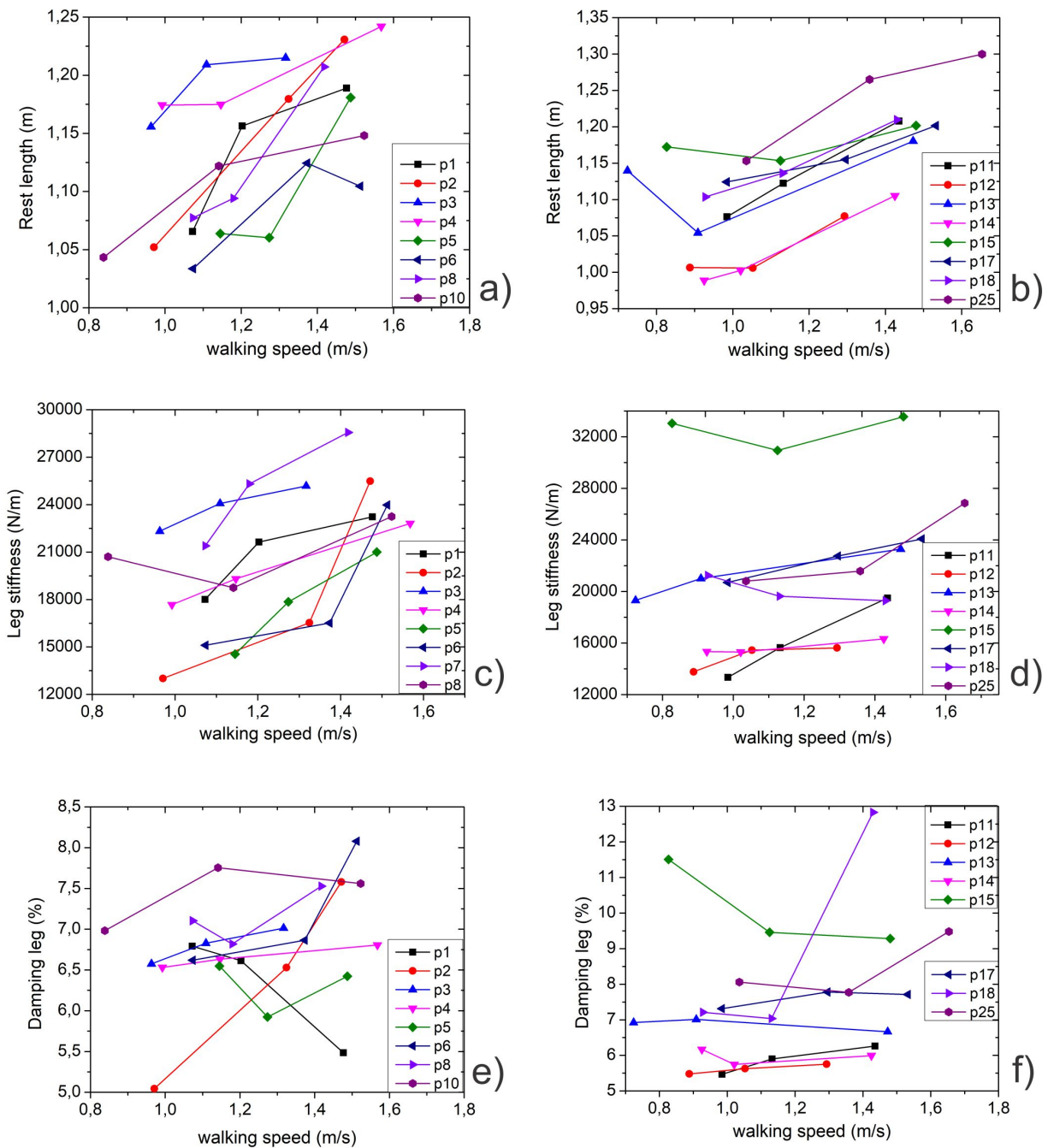


Figure 5. Variation of model parameters with walking speed, a)-b)Rest length of the leg, c)-d)leg stiffness and e)-f)damping leg

6 Conclusion

The present work utilized a comprehensive experimental data to identify the parameters of a bipedal walking model with springs and dampers. It is one of the few works that can be found in literature identifying parameters for a bipedal model related to experimental measures. The identification process through Monte Carlo simulations and quantification of errors allowed to find in an automatized way correlation of GRF as close as possible to experimental measures. The ranges of model parameters found are consistent with previous findings of other researchers providing confidence in the results.

A key limitation of this study is experimental data available only for rigid surface, and unmeasured forces in flexible structures where interaction between pedestrians and the vibrating structure can affect the GRF. However, the findings of this study are relevant to future research on HSI, and the suggested methodology can be extended to vibrating structures.

Acknowledgements

The authors acknowledge the financial support provided by the National Council for Scientific and Technological Development (CNPq).

References

- [1] Brownjohn, J., 1999. Energy dissipation in one-way slabs with human participation. *In: Proceedings of the Asia-Pacific Vibration Conference 99, Singapore*, vol. , pp. 155–60.
- [2] Qin, J. & Law, S., 2015. A three-dimensional human walking model. *Journal of Sound and Vibration*, vol. 357, pp. 437 – 456.
- [3] Da Silva, F., Brito, H., & Pimentel, R., 2013. Modeling of crowd load in vertical direction using biodynamic model for pedestrians crossing footbridges. *Canadian Journal of Civil Engineering*, vol. 40, n. 12, pp. 1196–1204.
- [4] Toso, M., Gomes, H., Da Silva, F., & Pimentel, R., 2016. Experimentally fitted biodynamic models for pedestrian–structure interaction in walking situations. *Mechanical Systems and Signal Processing*, vol. 72-73, pp. 590 – 606.
- [5] Shahabpoor, E., Pavic, A., & Racic, V., 2016. Identification of mass–spring–damper model of walking humans. *Structures*, vol. 5, pp. 233 – 246.
- [6] Bocian, M., Macdonald, J., & Burn, J., 2013. Biomechanically inspired modeling of pedestrian-induced vertical self-excited forces. *Journal of Bridge Engineering*, vol. 18, n. 12, pp. 1336–1346.
- [7] Dang, H. & Živanović, S., 2013. Modelling pedestrian interaction with perceptibly vibrating footbridges. *FME Transactions*, vol. 41, n. 4, pp. 271–278.
- [8] Whittington, B. & Thelen, D., 2009. A simple mass-spring model with roller feet can induce the ground reactions observed in human walking. *Journal of Biomechanical Engineering*, vol. 131, n. 1.
- [9] Qin, J., Law, S., Yang, Q., & Yang, N., 2013. Pedestrian–bridge dynamic interaction, including human participation. *Journal of Sound and Vibration*, vol. 332, n. 4, pp. 1107 – 1124.
- [10] Dang, H., 2014. *Experimental and Numerical Modelling of Walking Locomotion on Vertically Vibrating Low-Frequency Structures*. PhD thesis, University of Warwick.
- [11] Li, T., Li, Q., & Liu, T., 2019. An actuated dissipative spring-mass walking model: Predicting human-like ground reaction forces and the effects of model parameters. *Journal of Biomechanics*, vol. 90, pp. 58 – 64.
- [12] Faisca, R., 2003. *Caracterização de cargas geradas por atividades humanas*. PhD thesis, COPPE/UFRJ.
- [13] Vega, D., Magluta, C., & Roitman, N., 2016. Análise do comportamento de passarela sob a ação de cargas humanas. *Dissertação de mestrado*.
- [14] Kim, S. & Park, S., 2011. Leg stiffness increases with speed to modulate gait frequency and propulsion energy. *Journal of Biomechanics*, vol. 44, n. 7, pp. 1253 – 1258.